Orientation of Adsorbed Antibodies on Charged Surfaces by Computer Simulation Based on a United-Residue Model

ARTICLE *in* LANGMUIR · APRIL 2003

Impact Factor: 4.46 · DOI: 10.1021/la026871z

3 AUTHORS, INCLUDING:

Jian Zhou
South China University of Technology
84 PUBLICATIONS **1,593** CITATIONS

SEE PROFILE

Shengfu Chen
Zhejiang University
94 PUBLICATIONS **6,626** CITATIONS

SEE PROFILE

Orientation of Adsorbed Antibodies on Charged Surfaces by Computer Simulation Based on a United-Residue Model

Jian Zhou, Shengfu Chen, and Shaoyi Jiang*

Department of Chemical Engineering, University of Washington, Seattle, Washington 98195

Received November 19, 2002

In this work, we develop a new residue-based protein−surface interaction potential model. With this model, the adsorption and orientation of two antibodies, IgG1 and IgG2a, are studied by Monte Carlo simulations. Effects of surface charge density and sign, and solution ionic strength are examined in our simulations. Simulation results show that van der Waals and electrostatic interactions codetermine the orientation of adsorbed antibodies. At low surface charge density and high solution ionic strength, where van der Waals interactions dominate, both IgG1 and IgG2a exhibit multiple orientations. At high surface charge density and low solution ionic strength, where electrostatic interactions dominate, there are preferred orientations for these two antibodies on both positively and negatively charged surfaces, which are verified by experimental results. Due to a smaller dipole moment, IgG2a has more possible orientations than IgG1. IgG1 adsorbed on a positively charged surface shows an "end-on" orientation, which is well suited for biosensor applications. The simulation methodology and model could be directly applied to predict the adsorption and orientation of other proteins and to provide a fundamental understanding of their behavior on surfaces at the molecular level.

Introduction

The activity of an adsorbed enzyme or antibody depends on its orientation on a surface. The ability to control and manipulate antibody orientation behavior on a surface[1−3] is important to applications in biotechnology, clinical medicine, diagnostic assay, and environmental testing.

Various experimental approaches have been widely used to study the adsorption or immobilization of antibodies on a surface, including physical adsorption,[4−10] covalently coupling,[10−12] immobilization of F_{ab} via its native thiol,[13] attachment through a carbohydrate moiety in the F_c fragment,[14,15] and binding via protein A or protein G.[15,16] Among these methods, physical adsorption has its advantage that it is simple, and the adsorbed amount, orientation, and conformation of antibodies could be controlled upon adsorption by appropriately tuning various conditions. Physical adsorption is influenced by several factors, such as electrostatic interaction, van der Waals (VDW) interaction, hydrophobic effect, pH and ionic strength, and so forth. A fundamental understanding of these effects on the adsorption and orientation of antibodies on surfaces is of great importance to the development of biosensors.

Molecular simulation is well suited for providing insights about protein behavior on surfaces. Molecular simulation of proteins at interfaces could be carried out in three levels by colloid-bead, united-residue, and all-atom models. The simplest one is based on a colloid model, in which protein is modeled as a charged sphere[17−19] or as a combination of multiple beads proposed by us for a large nonspherical protein, such as an antibody.[20] Simulation studies of protein adsorption based on all-atom models were performed using Monte Carlo (MC),[21] molecular dynamics (MD),[22] and Brownian dynamics (BD)[23] simulation methods with solvent described as a continuous dielectric media. Only a simulation study of a small peptide, enkephalin, near a polyethylene surface[24] was reported with explicit water molecules. For the united-residue model, each amino acid residue is represented by one or a few interaction sites.[25−29] This model could be

* To whom correspondence should be addressed. E-mail: sjiang@u.washington.edu.

(1) Lu, B.; Smyth, M. R.; Kennedy, R. O. *Analyst* **1996**, *121*, 29R.
(2) Rao, S. V.; Anderson, K. W.; Bachas, L. G. *Mikrochim. Acta* **1998**, *128*, 127.
(3) Herron, J. N.; Wang, H. K.; Janatova, V.; Durtschi, J. D.; Caldwell, K. D.; Christensen, D. A.; Chang, I. N.; Huang, S. C. In *Biopolymers at Interfaces*; Marcel Dekker: New York, 1998; p 221.
(4) Bergkvist, M.; Carlsson, J.; Karlsson, T.; Oscarsson, S. *J. Colloid Interface Sci.* **1998**, *206*, 475.
(5) Buijs, J.; White, D. D.; Norde, W. *Colloids Surf., B* **1997**, *8*, 239.
(6) Buijs, J.; Lichtenbelt, J. W. T.; Norde, W.; Lyklema, J. *Colloids Surf., B* **1995**, *5*, 11.
(7) Buijs, J.; van den Berg, P. A. W.; Lichtenbelt, J. W. T.; Norde, W.; Lyklema, J. *J. Colloid Interface Sci.* **1996**, *178*, 594.
(8) Buijs, J.; Norde, W.; Lichtenbelt, J. W. T. *Langmuir* **1996**, *12*, 1605.
(9) Vermeer, A. W. P.; Giacomelli, C. E.; Norde, W. *Biochim. Biophys. Acta* **2001**, *1526*, 61.
(10) Wadu-Mesthrige, K.; Amro, N. A.; Liu, G. Y. *Scanning* **2000**, *22*, 380.
(11) Perez-Amodio, S.; Holownia, P.; Davey, C. L.; Price, C. P. *Anal. Chem.* **2001**, *73*, 3417.
(12) Vikholm, I.; Albers, W. M. *Langmuir* **1998**, *14*, 3865.
(13) Karyakin, A. A.; Presnova, G. V.; Rubtsova, M. Y.; Egorov, A. M. *Anal. Chem.* **2000**, *72*, 3805.
(14) Shriver-Lake, L. C.; Donner, B.; Edelstein, R.; Breslin, K.; Bhatia, S. K.; Ligler, F. S. *Biosens. Bioelectron.* **1997**, *12*, 1101.
(15) Vijayendran, R. A.; Leckband, D. E. *Anal. Chem.* **2001**, *73*, 471.
(16) Murata, M.; Arakawa, M.; Yoshida, T.; Hato, M. *Colloids Surf., B* **1998**, *12*, 35.
(17) Oberholzer, M. R.; Wagner, N. J.; Lenhoff, A. M. *J. Chem. Phys.* **1997**, *107*, 9157.
(18) Gray, J. J.; Bonnecaze, R. T. *J. Chem. Phys.* **2001**, *114*, 1366.
(19) Ravichandran, S.; Talbot, J. *Biophys. J.* **2000**, *78*, 110.
(20) Zhou, J.; Tsao, H. K.; Sheng, Y. J.; Jiang, S. Y. *Biophys. J.*, accepted.
(21) Juffer, A. H.; Argos, P.; DeVlieg, J. *J. Comput. Chem.* **1996**, *17*, 1783.
(22) Tobias, D. J.; Mar, W.; Blasie, J. K.; Klein, M. L. *Biophys. J.* **1996**, *71*, 2933.
(23) Ravichandran, S.; Madura, J. D.; Talbot, J. *J. Phys. Chem. B* **2001**, *105*, 3610.
(24) Bujnowski, A. M.; Pitt, W. G. *J Colloid Interface Sci.* **1998**, *203*, 47.
(25) Liwo, A.; Oldziej, S.; Pincus, M. R.; Wawak, R. J.; Rackovsky, S.; Scheraga, H. A. *J. Comput. Chem.* **1997**, *18*, 849.
(26) Liwo, A.; Pincus, M. R.; Wawak, R. J.; Rackovsky, S.; Oldziej, S.; Scheraga, H. A. *J. Comput. Chem.* **1997**, *18*, 874.
(27) Liwo, A.; Lee, J. Y.; Ripoll, D. R.; Pillardy, J.; Scheraga, H. A. *Proc. Natl. Acad. Sci.* **1999**, *96*, 5482.

10.1021/la026871z CCC: $25.00
Published on Web 03/21/2003

used to predict the native structures of proteins on the basis of sequence information. On the basis of this model, Dai et al.[30] developed an energy-based algorithm, POINTER, which can determine the permissible alignments of a polypeptide with respect to the lattice vectors of an interfacial surface. Besides molecular simulations, protein adsorption was also studied theoretically. Lenhoff and co-workers[31−35] systematically investigated protein−surface interaction energies by solving the Poisson−Boltzmann equation in both atomistic and colloidal frameworks. They found that negative adsorption free energy was dominated by a very small fraction of the configurations and electrostatic interaction was very important. Szleifer and co-workers[36,37] studied the kinetics and thermodynamics of protein adsorption by a generalized molecular theoretical approach. In addition, the lattice Monte Carlo method was used to study the adsorption of model proteins.[38,39] As to simulation studies of antibodies, attention was paid more to the antibody−antigen binding.[40−43]

Most previous simulation studies concentrated on interaction energy or adsorbed amount while little attention was paid to the orientation of adsorbed proteins. A practical problem in immunoassay applications is that progressively high coverage of IgGs on surfaces does not lead to strictly proportional changes in the antigen response of these surfaces, which highlights the difficulty of the preparation and control of dense and oriented biological films. Prediction and control of the orientation of adsorbed antibodies on surfaces is still challenging.

Due to the size of an antibody molecule, it is still prohibitive to perform molecular simulation of an all-atom antibody molecule in explicit solvent molecules on a surface. In our previous work, we used a simplified 12-bead model[20] to map out the orientation behavior of adsorbed antibodies under various surface and solution conditions. It provides useful information about the general trend of how various factors affect protein orientation on surfaces. However, the 12-bead model is oversimplified. To more realistically represent the antibody, we propose a united-residue model for an antibody in this work. A new residue-based protein−surface interaction potential model is developed. The adsorption and orientation of two antibodies, IgG1 and IgG2a, are studied by Monte Carlo simulations with this potential model. The effects of surface charge density and sign, and solution ionic strength on the orientation of adsorbed IgG1 and IgG2a are examined.

Protein−Surface Interaction Potential Model

The functions of a protein are connected with the amino acid residue sequence of the protein, so a united-residue model should be a good approximation to represent the structure of a protein molecule for molecular simulations. It has been found that the backbone and the interior side chains of a protein in solution are nearly the same as those in its crystal state.[44] Therefore, crystallographic structure is often assumed to be an adequate approximation to the structure in solution. The coordinates of many proteins are available from the Brookhaven Protein Data Bank (PDB). For IgG1 and IgG2a studied in this work, their PDB codes are 1IGY and 1IGT, respectively.

In our proposed united-residue model, each amino acid is reduced to a single sphere centered at the α-carbon position. Thus, the basic structure characters of two antibodies could still be kept. The protein structure is assumed rigid. Self-assembled monolayers (SAMs) are ideal platforms for protein adsorption studies[45−48] and biosensor applications.[49] Thus, we select a SAM as a model surface for the development of protein−surface interaction potential, which consists of both VDW and electrostatic interactions.

VDW Interactions. To obtain short-range VDW interactions between each amino acid residue and carboxyl-(or amino-) terminated SAMs, we first performed all-atom MC simulations to obtain the optimal orientation and distance of each residue on surfaces using the CHARMM force field.[50] The c(4 × 2) structures of $HS(CH_2)_{15}COOH$ and $HS(CH_2)_{15}NH_2$ SAMs with a 30° tilt angle on Au(111) surfaces were adopted. Sixty-four chains of thiols were used. With the optimal orientation fixed, each residue was moved away from or toward the surface from its optimal position and interaction energy was calculated at each distance. Thus, an interaction energy−distance curve was obtained. We fitted this curve with an empirical equation,

$$U(d) = 4\epsilon\left[\left(\frac{0.5\sigma}{d+\delta+0.5\sigma}\right)^{12} - \left(\frac{0.5\sigma}{d+\delta+0.5\sigma}\right)^{6}\right] \quad (1)$$

where d is the nearest distance between a residue and a surface; σ is the equivalent VDW diameter of each residue estimated from the VDW volume[51] of each residue; δ is a fitted size parameter, $\delta = 0.25$ Å; and ϵ is a fitted energy interaction parameter between one residue and a surface.

Two sets of VDW interaction parameters between 20 residues and 2 SAM surfaces were developed. They are listed in Table 1. As an example, the interaction energy between an aspartic acid (ASP) residue and an NH_2-terminated SAM surface is shown in Figure 1.

Electrostatic Interactions. As to the charge state of each residue in a protein, it is assumed that all arginine

(28) Liwo, A.; Kamierkiewicz, R.; Czaplewski, C.; Groth, M.; Oldziej, S.; Wawak, R. J.; Rackovsky, S.; Pincus, M. R.; Scheraga, H. A. *J. Comput. Chem.* **1998**, *19*, 259.
(29) Hassinen, T.; Perakyla, M. *J. Comput. Chem.* **2001**, *19*, 259.
(30) Dai, Y.; Evans, J. S. *J. Chem. Phys.* **2000**, *112*, 5144.
(31) Roth, C. M.; Lenhoff, A. M. *Langmuir* **1993**, *9*, 962.
(32) Johnson, C. A.; Wu, P.; Lenhoff, A. M. *Langmuir* **1994**, *10*, 3705.
(33) Roth, C. M.; Lenhoff, A. M. *Langmuir* **1995**, *11*, 3500.
(34) Asthagiri, D.; Lenhoff, A. M. *Langmuir* **1997**, *13*, 6761.
(35) Roth, C. M.; Sader, J. E.; Lenhoff, A. M. *J. Colloid Interface Sci.* **1998**, *203*, 218.
(36) Satulovsky, J.; Carignano, M. A.; Szleifer, I. *Proc. Natl. Acad. Sci.* **2000**, *97*, 9037.
(37) Fang, F.; Szleifer, I. *Biophys. J.* **2001**, *80*, 2568.
(38) Zhdanov, V. P.; Kasemo, B. *Proteins* **1998**, *30*, 168.
(39) Castells, V.; Yang, S. X.; van Tassel, P. R. *Phys. Rev. E* **2002**, *65*, 031912.
(40) Kozack, R. E.; d′Mello, M. J.; Subramaniam, S. *Biophys. J.* **1995**, *68*, 807.
(41) Davies, D. R.; Cohen, G. H. *Proc. Natl. Acad. Sci.* **1996**, *93*, 7.
(42) Gibas, C. J.; Subramaniam, S.; McCammon, J. A.; Braden, B. C.; Poljak, R. J. *Biochemistry* **1997**, *36*, 15599.
(43) Fogolari, F.; Ugolini, R.; Molinari, H.; Viglino, P.; Esposito, G. *Eur. J. Biochem.* **2000**, *267*, 4861.
(44) Wuthrich, K. *Science* **1989**, *243*, 45.
(45) Mrksich, M.; Whitesides, G. M. *Annu. Rev. Biophys. Biomol. Struct.* **1996**, *25*, 55.
(46) Prime, K. L.; Whitesides, G. M. *Science* **1991**, *252*, 1164.
(47) Ostuni, E.; Yan, L.; Whitesides, G. M. *Colloids Surf., B* **1999**, *15*, 3.
(48) Ostuni, E.; Chapman, R. G.; Holmlin, R. E.; Takayama, S.; Whitesides, G. M. *Langmuir* **2001**, *17*, 5605.
(49) Chaki, N. K.; Vijayamohanan, K. *Biosens. Bioelectron.* **2002**, *17*, 1.
(50) MacKerell, A. D., Jr.; Bashford, D.; Bellott, R. L.; Dunbrack, R. L., Jr.; Evanseck, J. D.; Field, M. J.; Fischer, S.; Gao, J.; Guo, H.; Ha, S.; Joseph-McCarthy, D.; Kuchnir, L.; Kuczera, K.; Lau, F. T. K.; Mattos, C.; Michnick, S.; Ngo, T.; Nguyen, D. T.; Prodhom, B.; Reiher, W. E., III; Roux, B.; Schlenkrich, M.; Smith, J. C.; Stote, R.; Straub, J.; Watanabe, M.; Wiorkiewicz-Kuczera, J.; Yin, D.; Karplus, M. *J. Phys. Chem. B* **1998**, *102*, 3586.
(51) Creighton, T. E. *Proteins: structures and molecular properties*, 2nd ed.; W. H. Freeman and Company: New York, 1993.

Table 1. Parameters for the Residue-Based Protein−Surface Interaction Potential Model

			ϵ/kJ·mol^{-1}	
residue	q/e	σ/Å	-COOH	-NH_2
ALA	0	5.039	9.696	9.367
ARG	1	6.563	13.127	11.105
ASN	0	5.681	10.931	13.921
ASP	−1	5.581	9.057	11.305
CYS	0	5.477	9.610	7.634
GLN	0	6.016	12.209	13.333
GLU	−1	5.927	10.666	8.236
GLY	0	4.509	8.414	9.459
HIS	0	6.086	10.003	12.747
ILE	0	6.187	12.937	10.688
LEU	0	6.187	7.632	7.583
LYS	1	6.365	11.310	10.156
MET	0	6.187	11.844	10.918
PHE	0	6.365	12.229	14.318
PRO	0	5.560	10.270	13.125
SER	0	5.185	7.633	10.907
THR	0	5.621	9.489	11.411
TRP	0	6.777	16.000	13.834
TYR	0	6.458	10.653	12.154
VAL	0	5.853	8.225	11.248

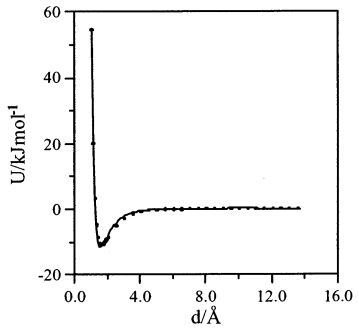

Figure 1. Residue−surface van der Waals interaction potential for ASP on an NH_2-terminated SAM. Results calculated on the basis of all-atom ASP with all-atom NH_2 SAMs are represented by dots, while results from the empirical equation (eq 1) are represented by the curve.

(ARG) and lysine (LYS) residues as well as the N-terminus are positively charged and all glutamic acid (GLU) and aspartic acid (ASP) residues along with the C-terminus are negatively charged. The pK_a of histidine (HIS) is around 6.0. At pH = 7.0, it is hardly protonated and is assumed to be neutral in this work. All other residues are neutral.

Due to the nonuniform distribution of charged residues, the whole protein has a dipole. The dipole moment of a protein, $\vec{\mu}$, is calculated by

$$\vec{\mu} = \sum_i [(\vec{R}_i - \vec{R}_{com})q_i] \qquad (2)$$

where $\vec{R}_i$ is the coordinate of each residue, $\vec{R}_{com}$ is the center of mass coordinate of a united-residue model protein, and q_i is the charge of each residue. The dipole moments of IgG1 and IgG2a studied are listed in Table 2. IgG1 shows a twisted-Y shape,[52] and the angle between the long axes of two F_{ab} fragments is 115°. IgG2a exhibits a compact T shape,[53] and the angle between the long axes of two F_{ab} fragments is close to 180°. The F_{ab} fragments are closer to the F_c fragment for IgG2a than for IgG1, and

Table 2. Some Properties of IgG1 and IgG2a

	PDB code	no. of residues	mol wt/ kDa	dipole moment/D	net charge/e
IgG1	1IGY	1294	143	3157	0
IgG2a	1IGT	1316	145	1374	0

the net charge in each fragment of IgG2a is less than that of IgG1, so the dipole moment of IgG2a is smaller.

By the aforementioned treatment of short-range VDW interactions between a protein and a surface, the substrate is reduced to a structureless plane. To consider the charge effect of the surface, uniform charge density on the surface is adopted. The electrostatic interaction[54−56] between a charged residue and the surface with uniform charge density is estimated by

$$U(z) = \frac{\sigma_s q_i e^{-\kappa z}}{\kappa \epsilon_0 \epsilon} \qquad (3)$$

where z is the distance between one residue and the surface, σ_s is the surface charge density, q_i is the charge of one residue, κ is the inverse Debye length calculated by $1/\kappa = 0.304/\sqrt{I}$ for a 1:1 salt,[54] I is the ionic strength, and ϵ_0 is the permittivity of free space. The effect of solvent is taken into account through the dielectric constant, ϵ = 78. The total electrostatic interaction energy is the summation of electrostatic interaction energies of all residues with the surface.

In contrast to the case of the all-atom representation, though this empirical residue−surface interaction model has some approximations, it provides a simple, yet reliable method for large-scale exploration of protein orientation on surfaces.

Simulation Details

Monte Carlo simulations were carried out in a box of 30 nm × 30 nm × 30 nm. The residue-based protein−surface interaction potentials were used. The temperature of the simulated system was 298 K. Only one antibody molecule was considered in simulations. Since the net charges of the two antibodies are both zero, the pH value of the simulated system corresponds to the isoelectric point of each antibody. Initially, the antibody was put 10 nm above the surface with a random orientation. During simulations, the protein was translated and rotated around its center of mass. The displacement of each move was adjusted to ensure an acceptance ratio of 0.5. At each condition, 10−30 simulations were performed to explore multiple orientations. Results reported in this study were usually averaged over two million configurations.

Results and Discussion

The adsorption and orientation of IgG1 and IgG2a on both positively charged and negatively charged surfaces are studied by MC simulations. The orientation angle is used to quantitatively characterize the orientation of the two antibodies on different charged surfaces. The orientation angle of an adsorbed antibody molecule is defined as the angle between the unit vector normal to the surface and the unit vector along the dipole of an antibody. Adsorption energies and average values of the cosine of the orientation angles of IgG1 and IgG2a at different

(52) Harris, L. J.; Skaletsky, E.; McPherson, A. *J. Mol. Biol.* **1998**, *275*, 861.
(53) Harris, L. J.; Larson, S. B.; Hasel, K. W.; McPherson, A. *Biochemistry* **1997**, *367*, 1581.
(54) Israelachvili, J. N. *Intermolecular and surface forces*, 2nd ed.; Academic Press: San Diego, CA, 1992.
(55) Hunter, R. J. *Foundations of Colloid Science*; Clarendon Press: Oxford, 1992; Vol. 1.
(56) Tsao, H. K. *J. Colloid Interface Sci.* **1998**, *202*, 527.

Table 3. Energies and Orientations of IgG1 on Positively Charged Surfaces

σ_s/C·m^{-2}	I/M	U/kJ·mol^{-1}	U_{VDW}/kJ·mol^{-1}	U_{ele}/kJ·mol^{-1}	cos θ	orientation	figure	P/%
0.006	0.005	−354.1	−63.4	−290.7	0.86	end-on	2a	100.00
	0.015	−220.7	−59.9	−160.8	0.86	end-on	2a	100.00
	0.1	−114.6	−78.5	−36.1	0.77	end-on	2b	100.00
	0.3	−92.0	−78.0	−14.0	0.77	end-on	2b	97.97
		−82.4	−80.6	−1.8	0.03	lying	2c	2.03
0.018	0.005	−948.0	−58.7	−889.3	0.86	end-on	2a	100.00
	0.015	−537.7	−53.5	−484.2	0.86	end-on	2a	100.00
	0.1	−187.8	−78.1	−109.7	0.77	end-on	2b	100.00
	0.3	−120.3	−78.5	−41.8	0.77	end-on	2b	100.00

Table 4. Energies and Orientations of IgG1 on Negatively Charged Surfaces

σ_s/C·m^{-2}	I/M	U/kJ·mol^{-1}	U_{VDW}/kJ·mol^{-1}	U_{ele}/kJ·mol^{-1}	cos θ	orientation	figure	P/%
−0.006	0.005	−295.9	−51.7	−244.2	−0.98	head-on	3a	100.00
	0.015	−159.1	−51.1	−108.0	−0.98	head-on	3a	100.00
	0.1	−79.6	−60.7	−18.9	−0.21	side-on	3b	98.88
		−68.5	−73.0	4.5	0.03	lying	3c	1.12
	0.3	−71.6	−73.3	1.7	0.03	lying	3c	91.54
		−65.7	−60.4	−5.3	−0.22	side-on	3b	8.46
−0.018	0.005	−784.3	−51.4	−732.9	−0.98	head-on	3a	100.00
	0.015	−376.1	−50.6	−325.5	−0.98	head-on	3a	100.00
	0.1	−117.2	−61.1	−56.1	−0.21	side-on	3b	100.00
	0.3	−76.6	−60.0	−16.6	−0.21	side-on	3b	97.52
		−67.5	−72.6	5.1	0.03	lying	3c	2.48

Table 5. Energies and Orientations of IgG2a on Positively Charged Surfaces

σ_s/C·m^{-2}	I/M	U/kJ·mol^{-1}	U_{VDW}/kJ·mol^{-1}	U_{ele}/kJ·mol^{-1}	cos θ	orientation	figure	P/%
0.006	0.005	−141.1	−90.3	−50.8	0.92	slanting	4c	92.97
		−134.7	−82.7	−52.0	0.38	lying	4d	7.03
	0.015	−108.3	−82.5	−25.8	0.38	lying	4d	99.34
		−94.4	−90.3	−4.1	0.92	slanting	4c	0.36
		−93.9	−80.8	−13.1	0.00	lying	4e	0.30
	0.1	−89.3	−88.4	−0.9	−0.10	lying	4f	54.94
		−87.5	−82.7	−4.8	0.38	lying	4d	26.57
		−86.4	−80.9	−5.5	0.00	lying	4e	17.04
		−80.3	−90.3	10.0	0.92	slanting	4c	1.45
	0.3	−93.7	−91.3	−2.4	−0.12	lying	4f	92.91
		−85.6	−82.9	−2.7	0.38	lying	4d	3.53
		−84.7	−90.1	5.4	0.92	slanting	4c	2.46
		−82.7	−80.8	−1.9	0.00	lying	4e	1.10
0.018	0.005	−255.2	−40.3	−214.9	0.77	end-on	4a	99.36
		−242.7	−90.5	−152.5	0.92	slanting	4c	0.64
	0.015	−160.3	−42.3	−118.0	0.52	end-on	4b	58.00
		−159.5	−81.0	−78.5	0.38	lying	4d	42.00
	0.1	−97.4	−81.0	−16.4	0.00	lying	4e	50.61
		−96.8	−82.1	−14.7	0.38	lying	4d	39.72
		−93.3	−83.7	−9.6	−0.08	lying	4f	9.67
	0.3	−97.7	−88.8	−8.9	−0.11	lying	4f	92.97
		−90.9	−82.7	−8.2	0.38	lying	4d	5.98
		−86.6	−80.9	−5.7	0.00	lying	4e	1.05

Table 6. Energies and Orientations of IgG2a on Negatively Charged Surfaces

σ_s/C·m^{-2}	I/M	U/kJ·mol^{-1}	U_{VDW}/kJ·mol^{-1}	U_{ele}/kJ·mol^{-1}	cos θ	orientation	figure	P/%
−0.006	0.005	−190.8	−58.1	−132.7	−0.94	side-on	5a	100.00
	0.015	−131.0	−80.2	−50.8	−0.49	head-on	5b	93.38
		−123.9	−57.6	−66.3	−0.94	side-on	5a	5.32
		−120.4	−53.9	−66.5	−0.02	slanting	5c	1.30
	0.1	−90.2	−80.2	−10.0	0.92	slanting	5d	52.84
		−89.5	−87.4	−2.1	−0.13	lying	5e	39.84
		−85.3	−79.3	−6.0	−0.48	head-on	5b	7.32
	0.3	−85.4	−80.0	−5.4	0.92	slanting	5d	55.83
		−84.6	−82.5	−2.1	−0.13	lying	5e	40.43
		−78.7	−79.3	0.6	−0.48	head-on	5b	3.74
−0.018	0.005	−456.3	−52.5	−403.8	−0.94	side-on	5a	100.00
	0.015	−259.0	−57.4	−201.6	−0.94	side-on	5a	91.54
		−253.1	−43.5	−209.6	−0.06	slanting	5c	8.46
	0.1	−113.8	−55.0	−58.8	−0.02	slanting	5c	80.41
		−110.3	−80.1	−30.2	0.92	slanting	5d	19.59
	0.3	−95.8	−79.5	−16.3	0.92	slanting	5d	99.61
		−81.3	−87.2	5.9	−0.14	lying	5e	0.29

surface and solution conditions are shown in Tables 3−6. The configurations of the two antibodies on positively and negatively charged surfaces are shown in Figures 2−5. In Figures 2−5, the two red circles in each configuration indicate the two antigen−antibody binding sites. In Tables 3−6, at each condition, there is a lowest-energy orienta-

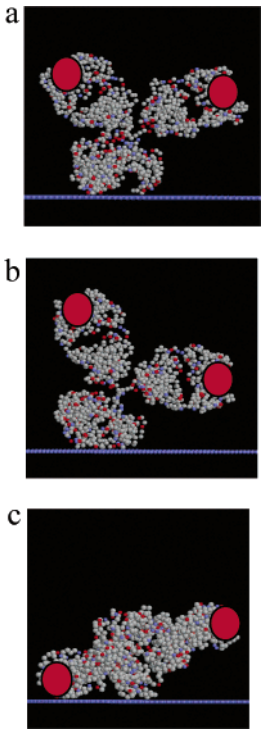

Figure 2. Typical orientations of IgG1 on positively charged surfaces.

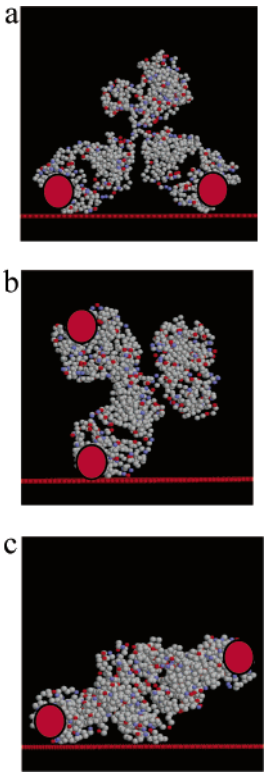

Figure 3. Typical orientations of IgG1 on negatively charged surfaces.

tion, which is most favorable. Roush et al.[57] calculated the interaction energy of rat cytochrome b5 on an anion-exchange adsorbent surface at discrete separation distances and orientations. Their results revealed the presence of a preferred orientation. In other studies, it was also found that protein−surface interaction energy

(57) Roush, D. J.; Gill, D. S.; Willson, R. C. *Biophys. J.* **1994**, *66*, 1290.

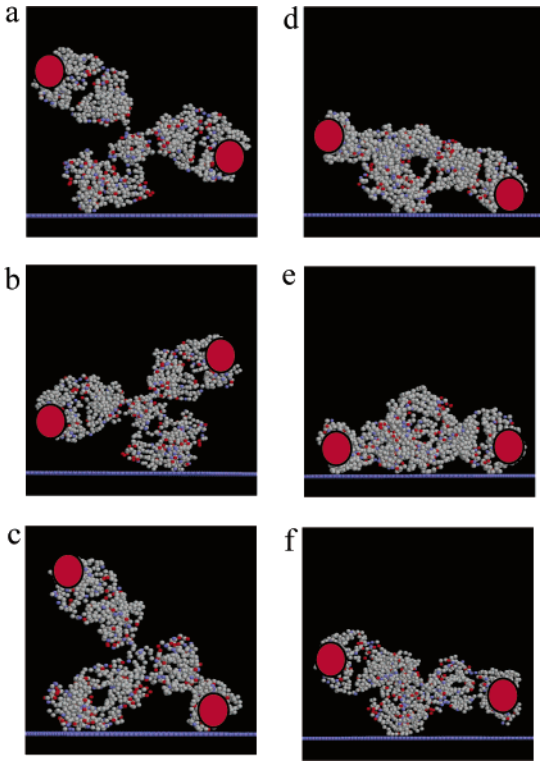

Figure 4. Typical orientations of IgG2a on positively charged surfaces.

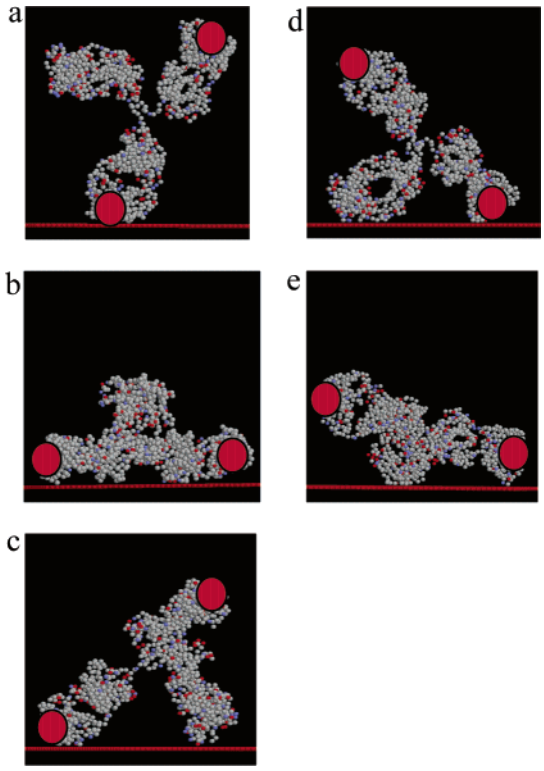

Figure 5. Typical orientations of IgG2a on negatively charged surfaces.

was dependent on protein orientation on the polymer surfaces.[58−60]

(58) Lu, D. R.; Park, K. *J. Biomater. Sci. Polym. Ed.* **1990**, *1*, 243.
(59) Lu, D. R.; Lee, S. J.; Park, K. *J. Biomater. Sci. Polym. Ed.* **1991**, *3*, 127.
(60) Noinville, V.; Vidal-Madjar, C.; Sebille, B. *J. Phys. Chem.* **1995**, *99*, 1516.

At some conditions, there exist multiple orientations for both IgG1 and IgG2a. The relationship between the probability of a specific configuration and its energy is

$$P_i = \frac{\exp(-U_i/kT)}{\sum_i \exp(-U_i/kT)} \quad (4)$$

U_i is the adsorption energy of configuration i, k is the Boltzmann constant, and T is the temperature. At 298 K, $1kT$ corresponds to 2.48 kJ·mol $^{-1}$. Any configuration whose adsorption energy is 17.1 kJ·mol^{-1} higher than the lowest one will be discarded, since the probability of appearance for this orientation will be less than 0.1%.

IgG1 on Positively Charged Surfaces. From Table 3 and Figure 2, it can be seen that at low ionic strengths, 0.005 M and 0.015 M, IgG1 on a positively charged surface has a typical "end-on" orientation, as shown in Figure 2a. At high ionic strengths, 0.1 M and 0.3 M, IgG1 on a positively charged surface mainly exhibits another "end-on" orientation, as shown in Figure 2b. The orientation shown in Figure 2b is very similar to that in Figure 2a, but with a 9° smaller orientation angle. The "lying" orientation shown in Figure 2c only appears at high ionic strength, 0.3 M, and low surface charge density, 0.006 C·m^{-2}. Under this condition, VDW interactions dominate and the behavior of adsorbed antibodies is similar to that on a neutral surface. Lu and Park[58] found that dispersion (VDW) attraction played a major role in protein adsorption on neutral polymer surfaces, which is consistent with our finding. Usually, IgG1 will have an "end-on" orientation on positively charged surfaces when electrostatic interactions dominate. This indicates that adsorbed IgG1 on positively charged surfaces is well suited for biosensor applications.

IgG1 on Negatively Charged Surfaces. From Table 4 and Figure 3, it can be seen that at low ionic strengths, 0.005 M and 0.015 M, IgG1 has a "head-on" orientation on a negatively charged surface, as shown in Figure 3a. The negatively charged surface repels the F_c fragment and attracts the F_{ab} fragments. This indicates that the antigen response should be very low, since binding sites are not accessible to antigens when the adsorbed antibody has a "head-on" orientation. Buijs et al.[5] studied antigen response using an adsorbed antibody on a negatively charged silicon surface, and they found that the antigen response was low. At high ionic strengths, 0.1 and 0.3 M, IgG1 has a "side-on" orientation, as shown in Figure 3b, with one of the Fab fragments on the surface. At a low surface charge density of −0.006 C·m^{-2} and high ionic strength, 0.3 M, where VDW interactions dominate, IgG1 exhibits a "lying" orientation, as shown in Figure 3c.

From our simulation results for IgG1 on positively and negatively charged surfaces, it is expected that IgG1 adsorbed on a positively charged surface would show a higher antigen response than that on a negatively charged surface. Our recent experiments with a surface plasmon resonance (SPR) biosensor[61] verify that IgG1 adsorbed on positively charged amino-terminated SAMs shows a higher antigen response than that on negatively charged carboxyl-terminated SAMs at low ionic strengths. Time-of-flight secondary ion mass spectrometry (ToF-SIMS)[62] results also show the tendency of the "head-on" orientation of IgG1 on carboxyl-terminated SAMs and the "end-on" orientation of IgG1 on amino-terminated SAMs, which agrees well with our simulation prediction.

IgG2a on Positively Charged Surfaces. From Table 5 and Figure 4, at a surface charge density of 0.018 C·m^{-2}, when ionic strength is as low as 0.005 M and 0.015 M, IgG2a shows "end-on" orientations, as shown in Figure 4a and b, respectively. Configurations 4a and 4b are similar except that the orientation angle of 4a is 20° closer to the vector perpendicular to the surface than that of 4b, due to larger electrostatic interactions. At low ionic strength, 0.005 M, when the surface charge density is 0.006 C·m^{-2}, IgG2a shows a "slanting" orientation, 4c, with the F_c fragment and one F_{ab} fragment on the positively charged surface. The direction of the dipole of IgG2a is pointing from the F_c fragment to another F_{ab} fragment. At the same ionic strength, 0.005 M, IgG2a displays orientations 4c and 4a, respectively on 0.006 and 0.018 C·m^{-2} surfaces, because stronger electrostatic interactions (due to higher surface charge density) will repel the F_{ab} fragments more away from the surface. For the same reason, at the same ionic strength, 0.015 M, IgG2a shows different preferred orientations, such as 4c and 4b, on 0.006 and 0.018 C·m^{-2} surfaces.

At high solution ionic strengths, 0.1 and 0.3 M, VDW interactions dominate. IgG2a has "lying" orientations on positively charged surfaces, as shown in Figure 4d−f. At low ionic strength, 0.015 M, and low surface charge density, 0.006 C·m^{-2}, IgG2a also shows a "lying" orientation, since VDW interactions dominate at this condition. The configurations shown in Figure 4d and f are very similar to each other except that different F_{ab} fragments are closer to the surface. The configurations shown in Figure 4e and f are both "lying" orientations, but with opposite sides of IgG2a facing the surface.

IgG2a on Negatively Charged Surfaces. From Table 6 and Figure 5, it can be seen that, at low ionic strength, 0.005 M, and surface charge density, −0.006 or −0.018 C·m^{-2}, or at 0.015 M and −0.018 C·m^{-2} conditions, IgG2a shows a "side-on" orientation (Figure 5a), with one F_{ab} fragment on the surface and another F_{ab} fragment pointing outward from the surface. Under these conditions, electrostatic interaction plays an important role. It is expected that there should be some antigen response for IgG2a adsorbed on a negatively charged surface. Our recent SPR experiments[61] show that antigen response for IgG2a on carboxyl-terminated SAMs is comparable to that on amino-terminated SAMs. At ionic strength 0.015 M and surface charge density −0.006 C·m^{-2}, IgG2a displays a "head-on" orientation, as shown in Figure 5b, since the electrostatic interaction of orientation 5b is not as strong as that of orientation 5a. At high ionic strengths, 0.1 and 0.3 M, where VDW interactions dominate, IgG2a has multiple orientations, as shown in Figure 5c−e.

When the orientations of IgG1 and IgG2a are compared at the same conditions, IgG1 has less orientations that are possible than IgG2a has on both positively and negatively charged surfaces. This is due to the larger dipole moment of IgG1 than that of IgG2a. Juffer et al.[21] found that close to the surface the mean force acting on the protein clearly varied with the strength of the dipole moment, and suggested a correlation between the dipole and the protein orientation with respect to the surface. However, only electrostatic interaction was considered in their work; this corresponds to the situation when electrostatic interactions dominate in our work. Ramsden et al.[63] studied the adsorption of two mutants of cytochrome

(61) Chen, S.; Liu, L.; Zhou, J.; Jiang, S. *Langmuir* **2003**, *19*, 2859.
(62) Wang, H.; Castner, D. G.; Ratner, B. D.; Jiang, S. *Langmuir*, submitted.
(63) Ramsden, J. J.; Roush, D. J.; Gill, D. S.; Kurrat, R.; Willson, R. C. *J. Am. Chem. Soc.* **1995**, *117*, 8511.

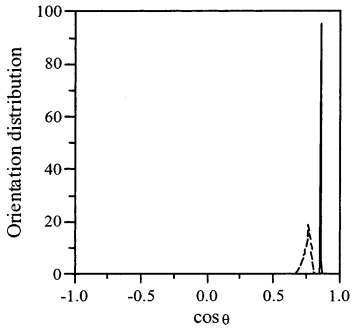

Figure 6. Orientation distributions of IgG1 and IgG2a on 0.018 $C \cdot m^{-2}$ positively charged surfaces at 0.005 M: solid line, IgG1; dashed line, IgG2a.

b5. They found that E15Q adsorbs with its major axis perpendicular to the surface, while E48Q has a more flexible adsorption mode due to the larger dipole moment of E15Q. In Figure 6, we show the orientation distribution of IgG1 and IgG2a at 0.005 M and 0.018 $C \cdot m^{-2}$. It is obvious that IgG1 shows a narrower distribution for a specific orientation than IgG2a does at the same solution and surface conditions, which is still due to the larger dipole moment of IgG1 than that of IgG2a.

It is well-known that electrostatic interaction plays an important role in ion-exchange chromatography and protein adsorption.[64] Ball et al.[65] measured the adsorption kinetics of lysozyme on a $Si(Ti)O_2$ surface. They found that the increases in adsorbed amount were linear with time at low ionic strength, 0.01 M, while the linear regime was not observed at high ionic strength, 0.15 M, suggesting an electrostatically driven self-assembled process at low ionic strength. This indicates that the adsorption kinetics of lysozyme is ionic strength-dependent. Ben-Tal et al.[66] found that the binding energy of small basic peptides to membranes decreases as salt concentration increases. Roth and Lenhoff[31] found that stronger electrostatic interactions enhanced the adsorbed amount of proteins and such an enhancement was most pronounced at low ionic strength. We observe the similar trend of the influence of electrostatic interaction on the orientation of adsorbed antibodies in this work; we find that the orientation of adsorbed antibodies is also ionic strength-dependent. For both IgG1 and IgG2a, at low ionic strength and high surface charge density conditions, preferred orientations are observed, since electrostatic interactions dominate. While at high ionic strength and low surface charge density conditions, multiple orientations were observed, since VDW interactions dominate. For both IgG1 and IgG2a, some orientations appear on both positively and negatively charged surfaces. For these cases, usually VDW interactions dominate. San Paulo et al.[67] obtained several high-resolution images of antibodies on mica using tapping-mode atomic force microscopy and found several morphologies, including "end-on", "head-on", "side-on", and "lying". They consider this phenomenon as a consequence of the nonspecific adhesion of antibodies on mica. Since the mica surface is weakly charged, electrostatic interaction is not strong, and VDW interaction dominates, multiple orientations are expected. This is in good agreement with our prediction.

Conclusions

In this work, we develop a new residue-based protein−surface interaction potential, which is more realistic than the 12-bead colloid model proposed previously and more computationally feasible than the all-atom model. It provides a simple, yet accurate method for the prediction of orientation of adsorbed proteins. Using this model, we perform Monte Carlo simulations to study the adsorption and orientation of two antibodies, IgG1 and IgG2a, on charged surfaces. Effects of surface charge density and sign, and solution ionic strength are examined in our simulations. Simulation results show that both van der Waals and electrostatic interactions codetermine the orientation of adsorbed antibodies. At low surface charge density and high solution ionic strength conditions, where the van der Waals interactions dominate, both IgG1 and IgG2a exhibit multiple orientations. Whereas at high surface charge density and low solution ionic strength conditions, where electrostatic interactions dominate, there is a corresponding preferred orientation for these two antibodies on both positively and negatively charged surfaces. Due to a smaller dipole moment, IgG2a has more orientations that are possible than IgG1 has. IgG1 adsorbed on a positively charged surface shows a desired "end-on" orientation at low ionic strength, which is well suited for biosensor applications.

The proposed mechanism, that is, electrostatically driven antibody orientation on charged surfaces, appears promising. It is consistent with most experimental results and can explain them reasonably. With our modeling work, it will be helpful to design surfaces with a desired orientation of adsorbed antibodies for biomaterial and biosensor applications. This work could also shed light on the mechanism for the orientation of all other adsorbed proteins at the molecular level.

Acknowledgment. The authors greatly acknowledge the Defense Advanced Research Projects Agency (F30602-01-2-0542) for financial support.

LA026871Z

(64) Honig, B.; Nicholls, A. *Science* **1995**, *268*, 1144.
(65) Ball, V.; Ramsden, J. J. *J. Phys. Chem. B* **1997**, *101*, 5465.
(66) Ben-Tal, N.; Honig, B.; Peitzsch, R. M.; Denisov, G.; McLaughlin. *Biophys. J.* **1996**, *71*, 561.
(67) San Paulo, A.; Garcia, R. *Biophys. J.* **2000**, *78*, 1599.